

Durham Research Online

Deposited in DRO:

24 October 2012

Version of attached file:

Published Version

Peer-review status of attached file:

Peer-reviewed

Citation for published item:

Abken, Anke E. and Halliday, D.P. and Durose, Ken (2009) 'Photoluminescence study of polycrystalline photovoltaic CdS thin film layers grown by close-spaced sublimation and chemical bath deposition.', *Journal of applied physics.*, 105 (6). 064515.

Further information on publisher's website:

<http://dx.doi.org/10.1063/1.3074504>

Publisher's copyright statement:

© 2009 American Institute of Physics. This article may be downloaded for personal use only. Any other use requires prior permission of the author and the American Institute of Physics. The following article appeared in Abken, Anke E. and Halliday, D.P. and Durose, Ken (2009) 'Photoluminescence study of polycrystalline photovoltaic CdS thin film layers grown by close-spaced sublimation and chemical bath deposition.', *Journal of applied physics.*, 105 (6) 064515 and may be found at <http://dx.doi.org/10.1063/1.3074504>

Additional information:

Use policy

The full-text may be used and/or reproduced, and given to third parties in any format or medium, without prior permission or charge, for personal research or study, educational, or not-for-profit purposes provided that:

- a full bibliographic reference is made to the original source
- a [link](#) is made to the metadata record in DRO
- the full-text is not changed in any way

The full-text must not be sold in any format or medium without the formal permission of the copyright holders.

Please consult the [full DRO policy](#) for further details.

Photoluminescence study of polycrystalline photovoltaic CdS thin film layers grown by close-spaced sublimation and chemical bath deposition

Anke E. Abken,^{1,2,a)} D. P. Halliday,² and Ken Durose²

¹*Institut für Solarenergieforschung GmbH, Hannover D-30165, Germany*

²*Physics Department, University of Durham, South Road, Durham DH1 3LE, United Kingdom*

(Received 18 June 2008; accepted 18 December 2008; published online 25 March 2009)

Photoluminescence (PL) measurements were used to study the effect of postdeposition treatments by annealing and CdCl₂ activation on polycrystalline CdS layer grown by close-spaced sublimation (CSS) and chemical bath deposition (CBD). CdS films were either annealed in a temperature range of 200–600 °C or CdCl₂ treated between 300–550 °C. The development of “red,” “intermediate orange,” “yellow,” and “green” luminescence bands is discussed in comparison with PL assignments found in literature. PL spectra from CdS layer grown by CSS are dominated by the yellow band with transitions at 2.08 and 1.96 eV involving (Cd_i-A), (V_S-A) complex states where A represents an acceptor. Green luminescence bands are observed at 2.429 and 2.393 eV at higher annealing temperature of 500–600 °C or CdCl₂ treatment above 450 °C, and these peaks are associated with zero and a longitudinal optical phonon replica of “free-to-bound” transitions. As grown CBD-CdS films show a prominent red band with four main peaks located at 1.43, 1.54, 1.65, and 1.77 eV, believed to be phonon replicas coupled with local vibrational modes. This remains following postdeposition treatment. The red luminescence is associated with V_S surface states and in the case of CdCl₂ treatment with (V_{Cd}-Cl_S) centers. Postdeposition treatments of CBD and CdS promote the evolution of an intermediate orange band at 2.00 eV, most likely a donor-acceptor pair, and a yellow band at 2.12 eV correlated with (Cd_i-V_{Cd}) centers. The green luminescence bands observed at 2.25 and 2.34 eV are associated with transitions from deep donor states (e.g., Cd_i) to the valence band. These states form due to crystallinity enhancement and lattice conversion during annealing or CdCl₂ activation. Observed changes in PL bands provide detailed information about changes in radiative recombination centers in CdS layer, which are suggested to occur during device processing of CdTe/CdS thin film solar cells. © 2009 American Institute of Physics. [DOI: 10.1063/1.3074504]

I. INTRODUCTION

Polycrystalline CdS films are used as *n*-type window layers in CdTe/CdS thin film heterojunction solar cells. A range of CdS deposition methods have been used for the preparation of efficient devices. However, two thin film preparation techniques dominate in this context: chemical bath deposition (CBD) and close-spaced sublimation (CSS). The highest efficiency small area solar cell devices have been achieved using CdS layers grown by CBD having record conversion efficiencies of 16.5%.^{1–3} The CSS technique allows large area deposition of CdS and CdTe films using high deposition rates. This technology was recently established for manufacturing of CdTe/CdS thin film solar modules.^{4,5}

In the superstrate configuration, CdTe/CdS solar cell devices involve the growth of polycrystalline CdS on transparent conductive coated glass followed by deposition of the CdTe absorber onto the CdS window layer. For efficient device formation, CdTe/CdS layer stacks are annealed under the influence of an “activation” agent CdCl₂ prior to back-contact application. A *p-n* heterojunction consisting of a

CdS_{1-x}Te_x interfacial layer between CdS and CdTe is formed during the high temperature CdTe deposition⁶ and the subsequent postdeposition CdCl₂ heat treatment.⁷ There is evidence that the optoelectronic properties of the CdS layer underneath the CdTe absorber are affected by the CdCl₂ annealing⁸ as well as by indiffusion of Te originating from CdTe and by ingress of other trace impurities.^{9–11} Similarly the diffusion of S into the CdTe alters the optoelectronic properties of the CdTe layer at the interface. There is evidence that the presence of a CdS_{1-x}Te_x interfacial layer resulting from interdiffusion of both S and Te produces more efficient photovoltaic (PV) devices¹² and references therein.

In this work we study the changes in CdS layers observed using low temperature photoluminescence (PL) measurements to investigate the optical properties of CSS and CBD grown layers and subsequently treated by annealing in nitrogen or CdCl₂. PL probes optically active recombination centers in CdS. Some of these will contribute to losses in photocurrent of solar cell devices due to optical absorption in the CdS window layer. PL can also provide information about impurity and defect centers which act as recombination centers for charge carriers which also reduces the PV conversion efficiency. It is known that the CdS material is highly compensated with comparable densities of shallow donor and deep acceptor states. Therefore, a portion of carriers, photogenerated in the *n*-CdS window layer, does not

^{a)}Author to whom correspondence should be addressed. Present address: First Solar, Inc., 28101 Cedar Park Boulevard, Perrysburg, OH 43551 (USA). Tel.: +1-419-662-7525. FAX: +1-419-662-8525. Electronic mail: anke.abken@gmx.net.

create photocurrent due to radiative and nonradiative recombination. In many cases solar cell device optimization is done empirically rather than systematically. Typically, this involves thinning the CdS in order to minimize absorption,¹³ reducing pin hole, or using CdCl₂ treatments of small-grained CdS prior to CdTe deposition.^{6,14–16}

Several papers have reported on PL studies performed on CdTe/CdS layer stacks.^{17–21} The evolution of PL peaks during device processing was correlated with the photovoltaic performance of devices.^{19,20} In general, PL peaks originating from CdTe are observed in the range of 1.3–1.5 eV. PL peaks related to CdS appear in the range of 1.9–2.2 eV. Further changes in the PL of CdS are due to the formation of a CdS_{1-x}Te_x interfacial layer by interdiffusion of Te during the CdCl₂ treatment. In some cases this can impact the entire thickness of the CdS layer. This creates broad PL emission bands in the range of 1.6–1.8 eV.²²

This paper focuses on PL measurement performed on polycrystalline CdS films and discusses the development of PL features according to deposition technique and postdeposition treatments relevant to CdTe/CdS device processing. This approach allows an in-depth understanding of the changes in the optoelectronic properties of the *n*-type CdS window layer, and how these changes are likely to occur during solar cell preparation. This study will support the future optimization of CdS films as window layers and will close the gap between theoretical and experimental conversion efficiencies achieved for CdTe/CdS thin film solar cell devices.

II. EXPERIMENTAL

A. CdS film deposition

CdS layers grown by CSS on In₂O₃:SnO₂/glass substrates (Merck–Balzers) were provided by ANTEC GmbH. The substrates were cleaned with Edisonit® and rinsed with ultrapure water prior to CdS deposition. CdS powder of 7N purity was used as source material. The substrate temperature was kept at 410 °C for a deposition time of 15 min; the CdS evaporation source was held at 715 °C.

Polycrystalline CdS layers were also grown on soda-lime glass and In₂O₃:SnO₂/glass (Merck–Balzers) substrates by CBD. The substrates were ultrasonically cleaned in a Mucsol® solution and rinsed with water before immersing them into a CdS deposition bath containing an aqueous solution of 9×10^{-4} m CdSO₄, 4.5×10^{-2} m (NH₂)₂CS, and NH₃. The bath was held at a temperature of 65 °C for a deposition time of 45 min.

B. Postdeposition annealing and CdCl₂ treatment

CdS samples were annealed for 1 h in a nitrogen atmosphere in a temperature range of 400–600 °C for CSS-CdS and between 200–500 °C for CBD-CdS, respectively. CdCl₂ activation treatments were performed by applying a CdCl₂ (Aldrich, 99.999%)/methanol solution (1 wt %) onto the CdS layers and followed by annealing for 1 h in a nitrogen atmosphere. Shorter annealing times comparable to those used for CdCl₂ processing of CdTe/CdS devices will lead to PL signals low in intensity; in order to achieve sufficient PL

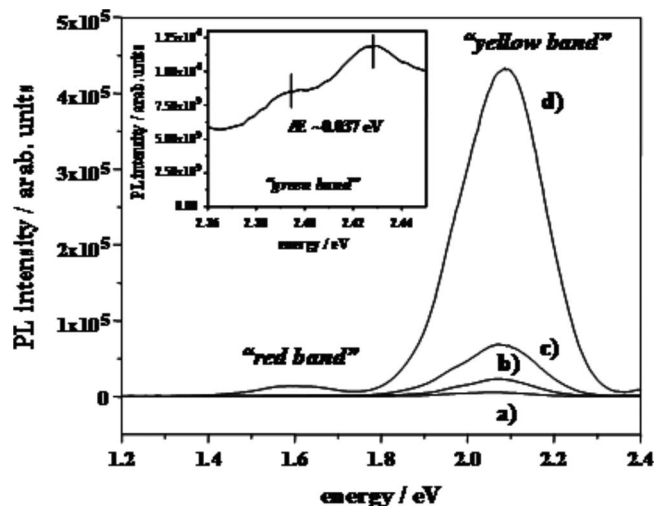


FIG. 1. PL spectra of CSS-CdS films: (a) as grown, (b) 400 °C, (c) 500 °C, and (d) 600 °C annealing in N₂ for 1 h. The inset shows green band for sample (d).

intensity the annealing time was increased to 1 h. The CdCl₂ annealing temperature range was 450–550 °C for CSS-CdS and 300–500 °C for CBD-CdS.

C. Photoluminescence measurements

The CdS samples were mounted into a closed-cycle helium cryostat, which was held at a temperature of 10 K. PL emission was excited by illuminating the samples from the film side using the 472.2 nm line of an argon ion laser providing an excitation density of between 4–10 mW cm⁻² on the sample surface.

Temperature dependent measurements were carried out by varying the temperature of the cryostat between 10 and 200 K.

III. RESULTS AND DISCUSSION

Low temperature PL measurements were performed on polycrystalline CdS films and recorded in a wavelength range between 510 and 1030 nm. There is an extensive literature on the luminescence of CdS. We have adopted a nomenclature, that is, wherever possible, consistent with the commonly used description of the different CdS PL emission bands. PL features appearing in the range of 2.18–2.54 eV, which is close to the band edge of CdS at 10 K, are called “green” bands; features appearing between 2.07 and 2.18 eV are typically referred to as “yellow” bands; the “orange” band is located between 2.00 and 2.07 eV, and luminescence observed around 1.54–2.00 eV is called the “infrared/red” band.

A. PL on CdS films grown by CSS

Figure 1 shows the PL spectra from CdS layers grown by CSS and after annealing the films in the temperature range of 400–600 °C. The inset shows the presence of the green band emission for a sample annealed at 600 °C in nitrogen. A broad feature in the yellow luminescence band dominates the PL spectrum. The yellow luminescence band exhibits a

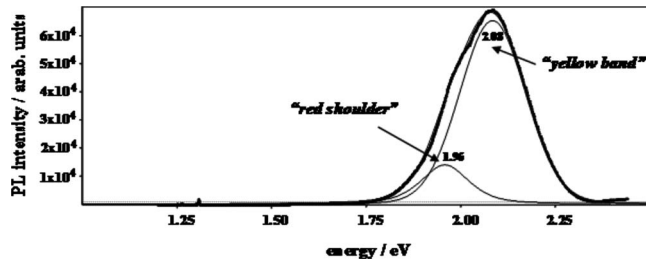


FIG. 2. PL spectrum and peak deconvolution for CSS-CdS layer annealed at 400 °C in N₂ for 1 h.

low energy asymmetry consisting of the superposition of a main PL peak centered at 2.08 eV and a smaller shoulder located at 1.96 eV in the red band. These transition energies were determined by Gaussian deconvolution of the spectra from a CdS sample annealed at 400 °C (see Fig. 2). The intensities of these two peaks were strongly dependent on annealing temperature. The intensity of the 2.08 eV peak increases with increasing temperature of the heat treatment. The red shoulder peak at 1.96 eV is only observed for samples annealed at 400 and 500 °C and vanishes at higher annealing temperatures of 600 °C. The yellow band becomes more prominent if the CdS films are coated with CdCl₂ before annealing in a temperature range of 450–550 °C for annealing times of about 1 h. The position

of the PL peaks observed for CdCl₂ treated samples is identical with the transition energy values found for annealed samples: 2.08 eV for the main feature and 1.96 eV for the satellite feature, and both peaks were observed for all CdCl₂ treated samples. Table I summarizes the PL features found for CSS-CdS layers as grown, annealed in nitrogen, and after CdCl₂ heat treatment.

The radiative transition observed at 2.08 eV is discussed in the literature as a donor-acceptor pair (DAP).²³ A donor level of 0.21 eV below the conduction band is suggested to be related to a cadmium interstitial Cd_i or to a sulfur vacancy V_S.²³ The acceptor level located 0.29–0.30 eV above the valence band^{23–25} is believed to originate from an impurity rather than from a native defect in CdS. Hong *et al.*²⁶ observe this transition at 2.09 eV. In contrast, some authors propose that the PL peak observed at 2.07 eV for Cd-rich CdS is caused by a “free-to-bound” transition from an unknown donor level located 0.51 eV below the conduction band to the valence band.^{27,28} The recombination of a free hole with an electron from native donor level, Cd_i or V_S, 0.11 eV below the conduction band leads to a green emission observed at 2.48 eV.²⁷ In our study the peak intensity of the band at 2.08 eV increases with annealing temperature or CdCl₂ treatment. This observation indicates that the 2.08 eV peak is more likely to be due to native defects of CdS.

TABLE I. Summary of PL bands found for CSS-CdS, as grown, N₂ annealed, and CdCl₂ treated.

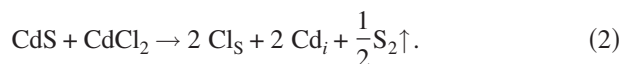
PL band	As grown	N ₂ annealed			CdCl ₂ treated			Origin	Reference
		400 °C	500 °C	600 °C	450 °C	500 °C	550 °C		
<i>Red band:</i>									
1.59–2.00 eV	1.59–1.60 eV	Not observed	Not observed	Weak	Medium			DAP with V _{Cd} and impurity level, e.g., Cl _S ;	[26,30,31]
	1.96 eV (shoulder peak of 2.08 eV band)	Not observed	Weak	Medium	Not observed			1.94 eV: E _{min} ; distant DAP with Cd _i or V _S and impurity related acceptor;	[29]
<i>Orange band:</i>									
2.00–2.07 eV		Not observed	Not observed in any sample;		Not observed in any sample;				
<i>Yellow band:</i>									
2.07–2.18 eV	2.08 eV	Dominant	Dominant; increases with annealing temperature;		Dominant; increases with treatment temperature;			2.08 eV: DAP with Cd _i or V _S donor (CB–0.21 eV) and impurity related acceptor (VB+0.29–0.30 eV);	[23–25,29]
								2.09 eV: DAP with Cd _i or V _S donor;	[26]
								2.07 eV: alternative donor (CB–0.51 eV) to VB transition; PL intensity increases in Cd over-pressure	[27,28]
									[23]
<i>Green band:</i>									
2.18–2.54 eV	>2.44 eV	Beyond detection limit;	Beyond detection limit;		Beyond detection limit;			2.536 eV: I1 transition of exciton bound to neutral acceptor;	[32,33]
	2.429 eV	Not observed	Not observed	Weak	Medium	Weak	Medium	2.425 eV (4.2 K): eA ^o or HES; ILO phonon replica;	[32–37]
	2.393 eV	Not observed	Not observed	Weak	Medium	Weak	Medium	ΔE=0.037 eV (4.2 K) 0.038eV (77 K);	[32,34,36]
								2.395 eV (4.2 K): DAP or LES;	[33–35,37]

Krustok²⁹ discusses the appearance of a shoulder peak at the low energy side of the dominating yellow band by considering the geometric distance between donor and acceptor in the CdS lattice. Transition energies of 2.08–1.94 eV were calculated for this transition as the DAP distance increases. This calculation suggests a large donor-acceptor separation for the defect associated with the 1.96 eV transition observed in our films. The difference of 120 meV between main and shoulder peak might be due to local phonon coupling.

Nevertheless, the contribution of Cd_i or V_S states to luminescence in the yellow band seems plausible from our observations. The intensity of the yellow band was reported to increase if the partial pressure of cadmium was raised during heat treatments of CdS single crystals.²³ In our case the increase in PL intensity of the yellow band during annealing of CdS films in a nitrogen atmosphere can be explained by loss in sulfur in CdS while increasing the concentration of Cd_i and V_S states,



Annealing under the influence of $CdCl_2$ promotes the formation of Cl_S states in addition to the increase in the Cd_i defect level concentration,



This model accounts for the increased PL intensity observed for the yellow luminescence of $CdCl_2$ treated CdS. Following this argument, the interpretation of the yellow luminescence at 2.08 eV with a shoulder peak at 1.96 eV as a donor-acceptor pair, (Cd_i -A) or (V_S -A), seems to be most likely.

A very small but broad feature centered at 1.6 eV in the red band is observed for CdS films annealed at temperatures above 500 °C. For $CdCl_2$ treated CdS the red luminescence is observed for all samples after annealing between 450 and 550 °C. It is proposed in the literature that these radiative transitions involve V_{Cd} and defect levels introduced by impurities,^{27,30,31} for $CdCl_2$ treated samples the involvement of Cl_S states³¹ seems to be most likely. However, the origin of red luminescence features in single crystals and well crystallized CdS layer is not fully understood.

Many papers describe the green luminescence for CdS single crystals,^{32–35} and several authors observe the green band for polycrystalline CdS films.^{36,37} In our study, we do not observe luminescence in the green band for as grown CSS-CdS films. A feature develops in this region only after higher temperature nitrogen (600 °C) or $CdCl_2$ treatment at 450 °C and higher and has a weak signal. The postdeposition heat treatment time of 1 h and high annealing temperatures compared to the short deposition time of 15 min during the CSS deposition process promote healing of structural defects and strain reduction in the CdS layer; overall, the crystallinity of the film improves, and this promotes green luminescence. $CdCl_2$ added to the CdS film before annealing acts as a fluxing agent and enhances recrystallization of CdS grains at low annealing temperatures.^{14,15}

The green band described in the literature for CdS single crystals is divided into a series of equally spaced lines. Lines related to excitons bound to neutral acceptors (“I1”) or donors (“I2”) are found to appear at 2.536 and 2.547 eV at 4.2 K.^{32,33} These lines are beyond the detection limit of 510 nm for the PL setup used in our study. At lower energies but still close to the “I” lines two additional series of PL peaks are observed for CdS crystals.^{32–34} The so-called “high emission series (HES)” is believed to arise from recombination of free electrons with holes bound to acceptors (free to bound or eA°) and is located typically at 2.425 eV (4.2 K). A “low emission series (LES)” originating from the recombination of electrons bound to donors with holes bound to acceptors (“bound to bound” or DAP) is centered at 2.395 eV (4.2 K).^{33–35,37} This feature is described for CdS single crystals and polycrystalline films.³⁶

In our case, a small peak centered at 2.429 eV (10 K) is observed developing in the green band after N_2 annealing at temperatures of 500–600 °C and after $CdCl_2$ treatment between 450 and 550 °C. The inset in Fig. 1 shows the green luminescence band for a sample N_2 annealed at 600 °C. This feature can be identified as a zero-phonon line of a free-to-bound transition. A second peak located at 2.393 eV might suggest a bound-to-bound transition. The low energy peak shows a lower intensity than the high energy peak, which indicates that the low energy peak is a longitudinal optical (1LO) phonon replica of the higher energy peak. The energy difference of ΔE 0.037 eV (10 K) between both peaks is in good agreement with values reported in the literature [$\Delta E = 0.037$ eV (4.2 K) for CdS single crystals].^{32,34} We do not observe any more than one phonon replica within the green band presumably due to the polycrystalline nature of CSS-CdS films. Furthermore, the low intensity of transitions makes a reliable identification of distinct lines correlated with the green luminescence band difficult. However, both N_2 annealing and $CdCl_2$ treatment promote the development of the green luminescence band in a similar way.

For evaporated CdS films Bleha and Peacock³⁶ discuss a PL peak of the green luminescence at 2.410 eV (77 K) as being the 1LO phonon replica with $\Delta E = 0.038$ V. Comparison of the green luminescence with measurements performed on CdS single crystals shows peak quenching and broadening for polycrystalline material, which was associated with the random orientation of grains and higher defect and impurity densities.³⁶ This is consistent with our measurements.

B. PL of CdS films grown by CBD

CBD allows the growth of small grained CdS films at low temperatures, typically between 60 and 85 °C. PL measurements reveal the dominance of a red band for CBD-CdS films grown on glass or $In_2O_3:SnO_2/glass$ substrates (Fig. 3). Table II summarizes the PL features found for CBD-CdS layers as grown, nitrogen annealed, and $CdCl_2$ treated. The red luminescence is still observed in PL spectra obtained for CdS films after heat treatment (Fig. 4) or $CdCl_2$ activation (Fig. 5). This band decreases in intensity with increasing annealing temperature. The red PL feature becomes less dominant after annealing CdS films at 500 °C, and this was

TABLE II. Summary of PL bands found for CBD-CdS deposited on glass¹ and In₂O₃:SnO₂/glass² as grown, N₂ annealed, and CdCl₂ treated.

PL band	As grown	N ₂ annealed				CdCl ₂ treated				Origin	Reference		
		200 °C	300 °C	400 °C	500 °C	300 °C	400 °C	450 °C	500 °C				
<i>Infrared band:</i>													
<1.59 eV	Not observed ^{a,b}	Not observed in any sample;				Not observed in any sample;				1.20–1.24 eV: V _{Cd} to VB;	[27,46]		
1.34 eV	Medium ^{a,b}	Weak ^a Medium ^b	Not observed ^a Medium ^b	Not observed ^{a,b}	Not observed ^{a,b}	Weak ^a Medium ^b	Medium ^{a,b}	Weak ^a Medium ^b	Not observed ^a Medium ^b				
1.43 eV	Dominant ^{a,b}	Dominant; decreasing with increasing annealing temperature ^{a,b}			Not observed ^{a,b}	Dominant; minor decrease with increasing treatment temperature ^a ; increasing with increasing treatment temperature ^b			Strong ^{a,b}				
<i>Red band:</i>													
1.59–2.00 eV	1.54 eV	Dominant ^{a,b}	Dominant; decreasing with increasing annealing temperature ^{a,b}			Medium ^a Weak ^b	Dominant; minor decrease with increasing treatment temperature ^a ; increasing with increasing treatment temperature ^b			Strong ^{a,b}	1.67–1.80 eV: surface state to VB; involvement of V _S ;	[30,31,38–41]	
	1.65 eV										[43,44,46]		
	1.77 eV	Dominant ^{a,b}		Medium ^a							1.69–1.72 eV: [V _S -Cl _S];	[30,31]	
	1.87 eV	Medium ^a Weak ^a	Medium ^{a,b}	Weak ^b	Medium ^{a,b}	Weak ^{a,b}		Medium ^{a,b}			1.83 eV: V _S to VB;	[46]	
<i>Orange band:</i>													
2.00–2.07 eV	2.00 eV	Not observed ^{a,b}	Not observed ^{a,b}	Increases with annealing temperature ^{a,b}		Dominant ^a Medium ^b	Not observed ^{a,b}	Not observed ^a Medium ^b	Medium ^{a,b}	DAP; not described in literature;			
<i>Yellow band:</i>													
2.07–2.18 eV	2.12 eV	Not observed ^{a,b}	Medium ^a Not observed ^a	Medium ^a Strong ^b	Medium ^{a,b}	Not observed ^{a,b}	Not observed ^a Medium ^b	Medium ^a Not observed ^b		2.11 eV: Cd _i involved, e.g., (Cd _i -V _{Cd}) formed during cubic to hexagonal transformation and S re-evaporation;		[39,43,44,47] [41,42]	
<i>Green band:</i>													
2.18–2.54 eV	2.25 eV	Not observed ^{a,b}	Not observed ^{a,b}		Strong ^a Dominant ^b	Not observed ^a Weak ^b	Not observed ^a	Not observed ^a Medium ^b	Not observed ^{a,b}	Medium ^a Weak ^b	2.2 eV: donor (Cd _i) to VB;		[39,43]
	2.34 eV	Not observed ^{a,b}	Not observed ^{a,b}		Strong ^a Dominant ^b		Not observed ^{a,b}	Not observed ^a Medium ^b	Not observed ^{a,b}	Dominant ^a Medium ^b	Shift from 2.25 to 2.34 eV due to band gap shift in CdS during cubic to hexagonal transformation;		[41,43]

^aReference 1.^bReference 2.

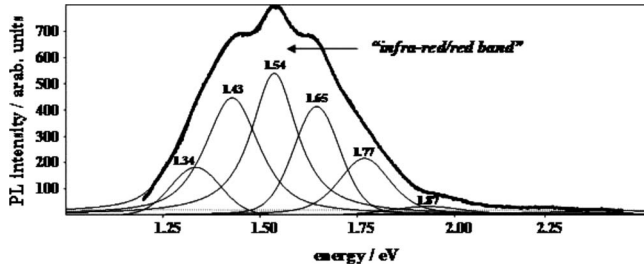


FIG. 3. PL spectrum and peak deconvolution for CBD-CdS layer as grown on $\text{In}_2\text{O}_3:\text{SnO}_2/\text{glass}$.

found independent of the substrate used for CdS deposition. For CdCl_2 activated samples the red band decreases less in its intensity with increasing treatment temperature than observed for annealed samples, but this was found only if glass substrates were used. In contrast, the intensity of the red luminescence increases with temperature for CdCl_2 treated CBD-CdS layer grown on $\text{In}_2\text{O}_3:\text{SnO}_2/\text{glass}$ (Fig. 5). In general, as grown CBD-CdS films deposited on glass and $\text{In}_2\text{O}_3:\text{SnO}_2/\text{glass}$ substrates show a distinct substructure of the red luminescence band, as shown in Fig. 3, for an as grown CBD-CdS film on $\text{In}_2\text{O}_3:\text{SnO}_2/\text{glass}$. Peak deconvolution and fitting the PL features with Gaussian curves reveal the existence of four main peaks centered at 1.43, 1.54, 1.65, and 1.77 eV, respectively. Adding less intense peaks at the low (1.34 eV) and high (1.87 eV) energy sides of the feature improves the fit. Heat treatment and CdCl_2 activation do not shift the peak positions significantly. The four main peaks of the red luminescence band show a constant energy separation of 100–110 meV, which is consistent with local phonon behavior. However, the energy separation is much higher than the energy of the LO (0.0377 eV), transversal optical (0.034 eV), and transversal acoustical (0.0206 eV) phonons in CdS.³² In our case we assume a coupling with local vibrational modes will account for the observed energy difference.

Red luminescence in polycrystalline and amorphous CdS films is described in the literature for layers grown by rf sputtering,³⁸ evaporation,^{39,40} or CBD.^{41–46} Depending on the growth method and CdS grain size the red luminescence is found centered at 1.67,⁴⁴ 1.7,^{31,39,40} 1.72,^{30,44} 1.77,³⁸ and 1.8 eV.^{43,46} It is believed that the red luminescence is caused by

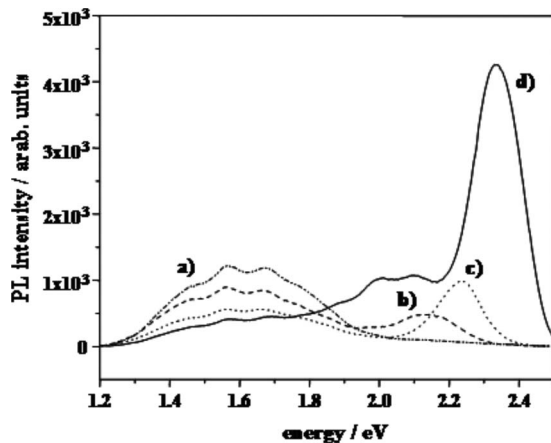


FIG. 4. PL spectra of CBD-CdS films grown on $\text{In}_2\text{O}_3:\text{SnO}_2/\text{glass}$ with annealing at (a) 200, (b) 300, (c) 400, and (d) 500 °C in N_2 for 1 h.

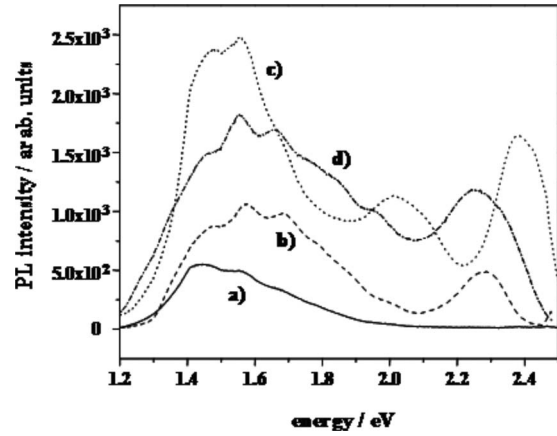


FIG. 5. PL spectra of CBD-CdS films grown on $\text{In}_2\text{O}_3:\text{SnO}_2/\text{glass}$ with CdCl_2 annealing at (a) 300, (b) 400, (c) 450, and (d) 500 °C in N_2 for 1 h.

transitions of electrons trapped in surface states to the valence band,^{39,40} and this effect is therefore correlated with the accumulation of crystallographic defects in CdS layers grown at low deposition temperatures. Annealing of small-grained CdS films increases grain size, decreases the number of grain boundaries, heals lattice defects, and reduces strain in the layer.^{38,39} As a result of the reduction in surface sites, a decrease in the red-band PL intensity is observed as recombination via these states becomes less significant. In general, the red emission band is associated with the involvement of sulfur vacancies in radiative recombination.^{41,44} Vigil *et al.*⁴⁶ describe luminescence observed at 1.83 eV with transitions from V_S^{2+} states to the valence band.

CdCl_2 has a significant effect on recrystallization of CBD-CdS grains and acts as a fluxing agent at low temperatures; we thus expected to see a reduction in the red luminescence with CdCl_2 treatment. We observed a smaller decrease in intensity of the red band than expected for this effect for CBD-CdS films grown on glass and an increase in red luminescence for CBD-CdS deposited on $\text{In}_2\text{O}_3:\text{SnO}_2/\text{glass}$ (Fig. 5). This suggests the formation of impurity related defect states^{30,31} leading to an increase in radiative recombination. Shiraki *et al.*³¹ discuss the appearance of red luminescence peak centered at 1.7 eV (4.2 K) with the formation of self-activated centers. These centers are based on a cadmium vacancy and a neighboring Cl_S state. If this is the case we expect that the ratio of surface defect density to self-activated ($V_{\text{Cd}}\text{-Cl}_S$) states determines the absolute values for the observed red PL intensity for CdCl_2 treated CdS films as CdCl_2 treatment is likely to introduce significant amounts of Cl into CdS films.

Some authors report the appearance of an infrared luminescence peak at 1.20²⁷ and 1.24 eV.⁴⁶ In our study, no evidence for the appearance of these PL bands was found.

Annealing CBD-CdS films at temperatures of 300 °C and higher or treating them with CdCl_2 at 400 °C and above promotes the development of an intermediate orange band centered at 2.00 eV, and this feature is typically accompanied by a yellow PL peak located at 2.12 eV (Figs. 6 and 7, Table II). The evolution of the orange and yellow luminescences is observed for CdS films grown on both glass and $\text{In}_2\text{O}_3:\text{SnO}_2/\text{glass}$ substrates, but these features are typically

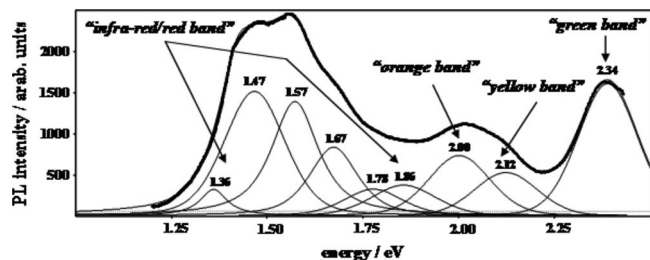


FIG. 6. PL spectrum and peak deconvolution for CBD-CdS layer grown on $\text{In}_2\text{O}_3:\text{SnO}_2/\text{glass}$ with CdCl_2 treatment at 450°C in N_2 for 1 h.

less pronounced for layers grown on glass. The intensity of both orange and yellow bands increases with annealing in a temperature range of $300\text{--}400^\circ\text{C}$. At high treatment temperatures of 500°C the intensity of the orange and yellow bands decreases in favor of the appearance of two green luminescence bands centered at 2.25 and 2.34 eV, which is observed for CBD-CdS/ $\text{In}_2\text{O}_3:\text{SnO}_2/\text{glass}$ samples exclusively. The PL spectra of CBD-CdS/glass structures annealed between 400 and 500°C were redominated by the intermediate orange band at 2.00 eV accompanied by the yellow PL peak at 2.12 eV (Fig. 7). Low intensity features in the green luminescence band appear due to annealing at 400°C located at 2.25 eV. Heat treatment at 500°C promotes the appearance of a PL peak at 2.34 eV. In PL spectra of CdCl_2 treated CBD-CdS films grown on $\text{In}_2\text{O}_3:\text{SnO}_2/\text{glass}$ the intermediate orange band at 2.00 eV and the yellow band at 2.12 eV are observed after CdCl_2 treatment of the films in a temperature range of $400\text{--}500^\circ\text{C}$. However, the intensities are lower than those observed for the green luminescence bands located at 2.25 and 2.34 eV. Yellow and orange luminescences appear for CdCl_2 treated CBD-CdS samples grown on glass at a treatment temperature of 500°C exclusively. However, orange and yellow PL features are observed along with the red and the green bands, and this was found independent of the substrate used for film deposition. In general CdCl_2 treatment seems to suppress the development of orange and yellow luminescences depending on the substrate used.

Some authors associate the yellow luminescence peak observed at 2.11 eV,^{43,47} those between $2.04\text{--}2.11$ eV,⁴⁴ and the green band at 2.20 eV with the formation of deep donor levels formed by Cd_i states.^{39,43} CdS layer grown by CBD typically appears amorphous in a metastable cubic crystal structure⁴¹ and in a mixed cubic and hexagonal structure⁴⁸ depending on processing parameters. These films transform

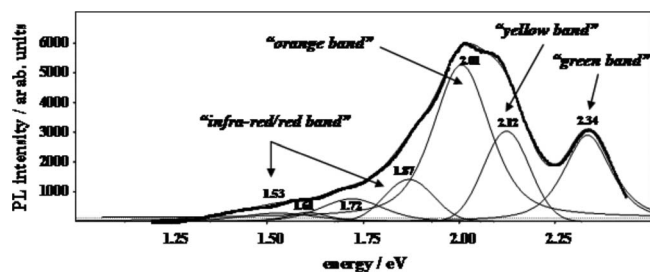


FIG. 7. PL spectrum and peak deconvolution for CBD-CdS layer grown on glass with annealing at 500°C in N_2 for 1 h.

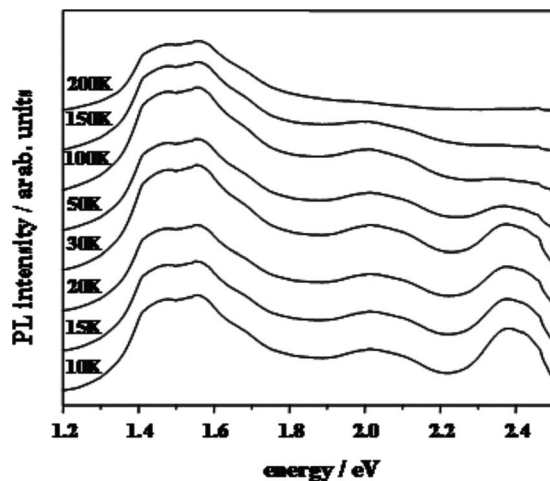


FIG. 8. Temperature dependent PL spectra of CBD-CdS layer grown on $\text{In}_2\text{O}_3:\text{SnO}_2/\text{glass}$ with CdCl_2 treatment at 450°C in N_2 for 1 h.

due to annealing in a temperature range of $240\text{--}300^\circ\text{C}$ into a stable hexagonal structure of CdS.^{41,48} Phase transformation is accompanied by rearrangement of native defects as well as by formation of defect complexes such as $(\text{Cd}_i\text{--}V_{\text{Cd}})$.⁴¹ Then, transitions from Cd_i donor levels to V_{Cd} acceptor levels are assumed to be the origin of yellow luminescence bands in annealed CdS films.^{41,42} As a result of the loss in sulfur, additional Cd_i and V_{Cd} defect levels are formed during annealing; CdCl_2 processing leads to sulfur re-evaporation and introduces Cl_i and Cd_i states in CdS. Thus, development of the yellow luminescence band is correlated with both effects: phase transformation and sulfur deficiency caused by heat treatment or CdCl_2 activation. Nevertheless, the chemical nature of defect states leading to the intermediate orange peak centered at 2.00 eV is unknown. The intensity of the intermediate orange luminescence band shows strong PL measurement temperature dependence; the PL intensity decreases with increasing temperature used for measurement until peak quenching occurs at temperatures above 150 K (Fig. 8). An activation energy of 129 meV was determined using an Arrhenius plot. The center of the peak shifts with temperature of the PL measurement with the same dependence observed for the band gap shift in CdS.⁴⁹ Overall, this behavior indicates that the intermediate orange band is presumably caused by a donor-acceptor recombination.

As mentioned above, N_2 -annealing at temperatures of 400°C and above on both types of substrate used in this study results in the development of intermediate orange (2.00 eV) and yellow (2.12 eV) bands and the evolution of a green band centered at 2.25 eV in CBD-CdS films (Figs. 4 and 5, Table II). Annealing at higher temperatures of 500°C can lead to the appearance of a second green luminescence band located at 2.34 eV. For CBD-CdS films grown on glass the PL feature observed at 2.25 eV vanishes in favor of the development of the 2.34 eV peak (Fig. 7). In contrast, CdS films grown on $\text{In}_2\text{O}_3:\text{SnO}_2/\text{glass}$ allow the coexistence of both green bands.

CdCl_2 treatment at 400°C promotes the development of green luminescence at 2.25 eV, and this is observed for CdS layers grown on $\text{In}_2\text{O}_3:\text{SnO}_2/\text{glass}$. The appearance of the

second green luminescence peak centered at 2.34 eV requires CdCl_2 treatments at 450 °C and above. The feature at 2.25 eV decreases in PL intensity with increasing treatment temperature with the band at 2.34 eV dominating the PL spectrum (Figs. 5 and 7). Using glass as substrate, high CdCl_2 treatment temperatures of 500 °C are necessary in order to promote both green luminescence bands.

However, for both substrates, glass and $\text{In}_2\text{O}_3:\text{SnO}_2/\text{glass}$ used for CBD-CdS deposition, the red luminescence band remains the most prominent feature up to CdCl_2 activation temperatures of 450 °C. The coexistence of the red band with the intermediate orange at 2.00 eV, the yellow PL band at 2.12 eV, and the green band at 2.34 eV was observed for CdS layer grown on $\text{In}_2\text{O}_3:\text{SnO}_2/\text{glass}$ after CdCl_2 treatment in a temperature range of 450–500 °C (Figs. 5 and 6).

Several studies report about the appearance of a PL feature located at 2.25 eV for CdS films grown by CBD^{43,45} and by sputtering,³⁸ respectively. Agata *et al.*³⁹ find this band centered around 2.2 eV for evaporated CdS films. It is believed that this luminescence band is caused by a transition from a donor level (e.g., Cd_i) to the valence band.^{39,43} As mentioned above, CdS films convert during heat treatment from a cubic into a hexagonal lattice structure. The lattice conversion is accompanied by rearrangement of donor and acceptor states as well as by an increase in CdS band gap provided these films are annealed at temperatures above 300 °C.⁴¹ In this case, the increase in CdS band gap leads to a shift in the green luminescence peak from 2.25 toward 2.34 eV when raising the annealing temperature from 400 up to 500 °C. The same effect is observed for CdCl_2 treated CdS layers deposited on $\text{In}_2\text{O}_3:\text{SnO}_2/\text{glass}$ substrates. Nevertheless, CdCl_2 treatment at high annealing temperatures seems to suppress lattice conversion of CdS grown directly on glass and presumably allows the coexistence of both lattice types, which is indicated by the appearance of both green luminescence bands, one feature centered at 2.25 eV and one peak found at 2.34 eV. In general, the intensity of green luminescence bands exhibits a strong dependence on the PL measurement temperature. Peak quenching was observed at temperatures of 150 K and above (Fig. 8) and an activation energy of 210 meV was determined for the second green band. The shift toward higher energies at higher PL measurement temperatures corroborates the assumption that the green luminescence is explained by a free-to-bound transition; there was no evidence for phonon replicas. We assume that this feature is caused by a defect level introduced by an impurity. However, the chemical nature of the impurity related defect state is unknown, but CBD is known to introduce non-negligible amounts of impurities into the films,^{50,51} which are likely to form recombination centers in CdS.

IV. CONCLUSION

CdS films grown by CSS and CBD exhibit differences in their optoelectronic properties during film growth and during postdeposition treatments such as annealing and CdCl_2 activation. These changes in material properties of CdS are suggested to have a non-negligible impact on the performance of

CdTe thin solar cell devices. Low temperature PL measurements provide a powerful tool for detecting defect states in CdS films provided these defect levels are involved in radiative recombination. However, interpretation of observed PL spectra may not be straightforward in every case, but the approach adopted in this work provides important information about recombination centers and their changes due to processing in polycrystalline CdS.

PL spectra of CdS films grown by CSS are dominated by a yellow band, a superposition of a main luminescence peak centered at 2.08 eV, and a red shoulder peak located at 1.96 eV. Donor-acceptor pairs, ($\text{Cd}_i\text{-A}$) and ($\text{V}_s\text{-A}$), are suggested to be responsible for these transitions. CSS-CdS films become sulfur deficient during annealing in N_2 and CdCl_2 activation, which increases the Cd_i and V_s defect density leading to an increase in PL intensity of the yellow luminescence. Green luminescence bands associated with zero phonon and 1LO replicas of free-to-bound (eA^0) transitions located at 2.429 and 2.393 eV develop after annealing CSS-CdS films with or without CdCl_2 at high temperatures.

PL spectra of CdS layers grown by CBD are dominated by a broad red luminescence band, a zero-phonon transition with phonon replicas resulting from local vibrational modes. Transitions of the red band are observed on films as grown, after N_2 annealing, or CdCl_2 treatment and involve surface states or in the case of CdCl_2 treatment self-activated ($\text{V}_{\text{Cd}}\text{-Cl}_s$) centers. High temperature postdeposition treatment of CBD-CdS films grown on $\text{In}_2\text{O}_3:\text{SnO}_2/\text{glass}$, N_2 annealing at temperatures higher than 300 °C, or CdCl_2 treatment at temperatures of 400 °C and above all promote the development of an intermediate orange band located at 2.00 eV, a yellow band at 2.12 eV, and two green bands centered at 2.25 and 2.34 eV. These bands appear in CBD-CdS layers grown directly on glass in the same temperature range used for N_2 annealing while CdCl_2 treatment inhibits the development of these features up to annealing temperatures of 500 °C. The intermediate orange PL feature centered at 2.00 eV indicates a donor-acceptor recombination and the yellow band observed at 2.12 eV is correlated with ($\text{Cd}_i\text{-V}_{\text{Cd}}$) complexes. Deep donor Cd_i state density increases due to sulfur deficiency of CdS after N_2 annealing or CdCl_2 activation and due to phase transformation of CBD-CdS from cubic to hexagonal during annealing at temperatures above 300 °C. Green luminescence bands centered at 2.25 and 2.34 eV are suggested to be transitions from donor levels (e.g., Cd_i states) to the valence band. An increase in band gap due to lattice conversion from cubic to hexagonal may account for the observed shift in the green PL peak toward higher energies. A significant annealing temperature difference for developing PL features of the yellow, orange, and green luminescences is indicated between CBD-CdS layers grown on $\text{In}_2\text{O}_3:\text{SnO}_2/\text{glass}$ and glass substrates; the impact of the substrate used for CBD-CdS film growth becomes more evident during CdCl_2 treatment.

Overall, this work contributes substantially to our knowledge on the optoelectronic properties of CdS films grown by techniques, which are successfully used for preparation and manufacturing of high efficiency CdTe/CdS solar cell devices. Special emphasis was focused on changes in the

defect structure of CdS, which are likely to occur during postdeposition treatments such as annealing and CdCl₂ activation. The increase in *n*-type doping of polycrystalline CdS films and resolving the problem of collection losses in CdS are key objectives of engineering CdS window layers forming a heterojunction with the *p*-CdTe absorber. These issues are of significant importance for the optimization of CdTe thin film solar cells providing improved long-term performance.

ACKNOWLEDGMENTS

ANTEC GmbH, Kelkheim (Germany) is gratefully acknowledged for providing CSS-CdS substrates. The authors would like to thank J. D. Russell and R. Curtis, University of Durham (U.K.), for performing the PL measurements. This study was financially supported by the Bundesministerium für Bildung, Wissenschaft und Technologie BMWi (Contract No. 0329787), and the European Union (Contract No. JOR 3980218; "Cadback").

- ¹C. S. Ferekides, J. Britt, Y. Ma, and L. Killian, Proceedings of the 23rd IEEE PV Specialists Conference, Louisville, 1993, p. 389 (unpublished).
- ²X. Wu, J. C. Keane, R. G. Dhere, C. DeHart, D. S. Albin, A. Duda, T. A. Gessert, S. Asher, D. H. Levi, and P. Sheldon, Proceedings of the 17th EU PV Solar Energy Conference, Munich, 2001, p. 995 (unpublished).
- ³X. Wu, *Sol. Energy* **77**, 803 (2004).
- ⁴D. Bonnet, *Thin Solid Films* **361–362**, 547 (2000).
- ⁵M. Harr and D. Bonnet, Proceedings of the 17th EU PV Solar Energy Conference, Munich, 2001, p. 1001 (unpublished).
- ⁶C. S. Ferekides, D. Marinsky, V. Viswanathan, B. Tetali, V. Palekis, P. Salvaraj, and D. L. Morel, *Thin Solid Films* **361–362**, 520 (2000).
- ⁷B. E. McCandless and S. S. Hegedus, Proceedings of the 22nd IEEE PV Specialists Conference, Las Vegas, 1991, p. 967 (unpublished).
- ⁸J. Kokaj and A. E. Rakhshani, *J. Phys. D* **37**, 1970 (2004).
- ⁹M. Emziane, K. Durose, D. P. Halliday, N. Romeo, and A. Bosio, *J. Appl. Phys.* **97**, 114910 (2005).
- ¹⁰M. Emziane, K. Durose, D. P. Halliday, N. Romeo, and A. Bosio, *Semicond. Sci. Technol.* **20**, 434 (2005).
- ¹¹K. Durose, M. A. Cousins, D. S. Boyle, J. Beier, and D. Bonnet, *Thin Solid Films* **403–404**, 396 (2002).
- ¹²D. Bonnet, Proceedings of the 19th EU PV Solar Energy Conference, Paris, 2004, p. 1657 (unpublished).
- ¹³C. S. Ferekides, U. Balusubramanian, R. Mamazza, V. Viswanathan, H. Zhao, and D. L. Morel, *Sol. Energy* **77**, 823 (2004).
- ¹⁴N. Romeo, A. Bosio, R. Tedschedi, A. Romeo, V. Canevari, and D. Leone, Proceedings of the 14th EU PV Solar Energy Conference, Barcelona, 1997, p. 2351 (unpublished).
- ¹⁵N. Romeo, A. Bosio, R. Tedschedi, A. Romeo, and V. Canevari, *Mater. Chem. Phys.* **66**, 201 (2000).
- ¹⁶S. C. Park, B. W. Han, J. H. Ahn, B. T. Ahn, and D. Kim, Proceedings of the 26th IEEE PV Solar Energy Conference, Anaheim, 1997, p. 531 (unpublished).
- ¹⁷D. P. Halliday, J. M. Eggleston, and K. Durose, *J. Cryst. Growth* **186**, 543 (1998).
- ¹⁸D. P. Halliday, J. M. Eggleston, and K. Durose, *Thin Solid Films* **322**, 314 (1998).
- ¹⁹M. D. G. Potter, D. P. Halliday, M. Cousins, and K. Durose, *Thin Solid Films* **361–362**, 248 (2000).
- ²⁰M. D. G. Potter, D. P. Halliday, and M. Cousins, Proceedings of the 16th EU PV Solar Energy Conference, Glasgow, 2000, p. 847 (unpublished).
- ²¹M. A. Hernández-Fenollosa, D. P. Halliday, K. Durose, M. Campo, and J. Beier, *Thin Solid Films* **431–432**, 176 (2003).
- ²²D. H. Levi, B. D. Fluegel, R. K. Ahrenkiel, A. D. Compaan, L. M. Woods, D. H. Rose, R. J. Matson, and D. S. Albin, Proceedings of the 25th IEEE PV Specialists Conference, Washington, 1996, p. 913 (unpublished).
- ²³K. Mochizuki, M. Satoh, and K. Igaki, *Jpn. J. Appl. Phys., Part 1* **22**, 1414 (1983).
- ²⁴G. H. Hershman and F. A. Kröger, *J. Solid State Chem.* **2**, 483 (1970).
- ²⁵R. Boyn, O. Goede, and S. Kushner, *Phys. Status Solidi* **12**, 57 (1965).
- ²⁶K. J. Hong, T. S. Jeong, C. J. Yoon, and Y. J. Shin, *J. Cryst. Growth* **218**, 19 (2000).
- ²⁷N. Susa, H. Watanabe, and M. Wada, *Jpn. J. Appl. Phys., Part 1* **15**, 2365 (1976).
- ²⁸I. Uchida, *J. Phys. Soc. Jpn.* **21**, 645 (1966).
- ²⁹J. Krustok, *J. Phys. Chem. Solids* **53**, 1027 (1992).
- ³⁰M. Yamaguchi, *Jpn. J. Appl. Phys., Part 1* **15**, 1675 (1976).
- ³¹Y. Shiraki, T. Shimada, and K. F. Komatsubara, *J. Appl. Phys.* **45**, 3554 (1974).
- ³²D. G. Thomas and J. J. Hopfield, *Phys. Rev.* **128**, 2135 (1962).
- ³³K. Maeda, *J. Phys. Chem. Solids* **26**, 1419 (1965).
- ³⁴K. Colbow, *Phys. Rev.* **141**, 742 (1966).
- ³⁵C. H. Henry, R. A. Faulkner, and K. Nassau, *Phys. Rev.* **183**, 798 (1969).
- ³⁶W. P. Bleha and R. N. Peacock, *J. Appl. Phys.* **41**, 4992 (1970).
- ³⁷J. Conradi, *Can. J. Phys.* **47**, 2591 (1969).
- ³⁸C. T. Tsai, D. S. Chuu, G. L. Chen, and S. L. Yang, *J. Appl. Phys.* **79**, 9105 (1996).
- ³⁹M. Agata, H. Kurase, S. Hayashi, and K. Yamamoto, *Solid State Commun.* **76**, 1061 (1990).
- ⁴⁰T. Arai, T. Yoshida, and T. Ogawa, *Jpn. J. Appl. Phys., Part 1* **26**, 396 (1987).
- ⁴¹R. Lozada-Morales and O. Zelaya-Angel, *Thin Solid Films* **281–282**, 386 (1996).
- ⁴²L. Hernández, O. de Melo, O. Zelaya-Angel, R. Lozada-Morales, and E. Purón, *J. Electrochem. Soc.* **141**, 3238 (1994).
- ⁴³H. Ariza-Calderon, R. Lozada-Morales, O. Zelaya-Angel, J. G. Mendoza-Alvarez, and L. Baños, *J. Vac. Sci. Technol. A* **14**, 2480 (1996).
- ⁴⁴J. Aguilar-Hernández, G. Contreras-Puente, A. Morales-Acevedo, O. Vigil-Galán, F. Cruz-Gandarilla, J. Vidal-Larramendi, A. Escamilla-Esquivel, H. Hernández-Contreras, M. Hesiquio-Garduño, A. Arias-Carbajal, M. Chavarría-Castañeda, and G. Arriaga-Mejía, *Semicond. Sci. Technol.* **18**, 111 (2003).
- ⁴⁵M. Gracia-Jiménez, G. Martínez, J. L. Martínez, E. Gómez, and A. Zehe, *J. Electrochem. Soc.* **131**, 2974 (1984).
- ⁴⁶O. Vigil, I. Riech, M. Garcia-Rocha, and O. Zelaya-Angel, *J. Vac. Sci. Technol. A* **15**, 2282 (1997).
- ⁴⁷C. Mejía-García, A. Escamilla-Esquivel, G. Contreras-Puente, M. Tufiño-Velázquez, M. L. Albor-Aguilera, O. Vigil, and L. Vaillant, *J. Appl. Phys.* **86**, 3171 (1999).
- ⁴⁸H. Metin and R. Esen, *J. Cryst. Growth* **258**, 141 (2003).
- ⁴⁹Y. P. Varshni, *Physica (Amsterdam)* **34**, 149 (1967).
- ⁵⁰A. Kylner, J. Lindgren, and L. Stolt, *J. Electrochem. Soc.* **143**, 2662 (1996).
- ⁵¹A. Kylner and E. Niemi, Proceedings of the 14th EU PV Solar Energy Conference, Barcelona, 1997, p. 1326 (unpublished).